Low-energy electron diffraction study of the growth of ultrathin films of face-centred cubic Co on Rh(001)

1993 J. Phys.: Condens. Matter 5 7307

(http://iopscience.iop.org/0953-8984/5/40/006)

J. Phys.: Condens. Matter 5 (1993) 7307–7318. Printed in the UK

Low-energy electron diffraction study of the growth of ultrathin films of face-centred cubic Co on Rh{001}

A M Begley†, S K Kim†, F Jona† and P M Marcus‡

† Department of Materials Science and Engineering, State University of New York, Stony Brook, NY 11794-2275, USA

‡ IBM Research Center, Yorktown Heights, NY 10598, USA

Received 21 May 1993, in final form 5 August 1993

Abstract. The epitaxial growth of Co on Rh{001} at room temperature is studied by means of quantitative low-energy electron diffraction and Auger electron spectroscopy. The Co films are found to grow pseudomorphic to the substrate in the layer-by-layer mode for at least two layers. The interlayer spacing between the monolayer and the substrate is 1.77 ± 0.03 Å. The first and second interlayer spacings for a bilayer film are 1.60 ± 0.04 and 1.75 ± 0.04 Å, respectively. Strained pseudomorphic films of up to 10 layers could be grown with a bulk lattice spacing of 1.60 ± 0.03 Å and a 3.1%-expanded first interlayer spacing (1.65 ± 0.03 Å). An elastic strain analysis shows that the equilibrium (unstrained) phase of these Co films is face-centred cubic: the bulk interlayer spacing is contracted by 9.7% with respect to the equilibrium value (1.772 Å) as a consequence of the large positive planar epitaxial strain produced by the 7.3% lattice mismatch between FCC Co and Rh.

1. Introduction

Ultrathin films of cobalt have attracted great interest in recent years both for their technological applications in magnetic multilayer systems [1–5] and for their ability to stabilize, through epitaxy, structures that do not occur naturally at room temperature, i.e. the metastable face-centred cubic (FCC) phase [6–8] and the metastable body-centred cubic (BCC) phase [9–11]. The former was found to grow on both Cu{001} [6–8] and Ni{001} [9]: the small mismatch between the lattice constants (+2.0% for Co/Cu and −0.6% for Co/Ni) allows the growth of thick epitaxial pseudomorphic films. Metastable BCC Co was grown by molecular beam epitaxy on GaAs{110} [10, 11] (mismatch −0.1%) and by standard procedures on Fe{001} [12] (mismatch +1.3%) and on Cr{001} [13] (mismatch +1.9%).

This paper reports an extensive study of the growth of Co on one of the few transition metal surfaces so far not utilized as a substrate, namely FCC Rh{001}. The room-temperature lattice constant of Rh is 3.804 Å [14], hence the edge of the primitive unit mesh on a {001} surface is 2.69 Å. The lattice constant of the metastable FCC phase of Co at room temperature is 3.544 Å [14], hence the sides of the primitive unit mesh on {001} are 2.506 Å long—the misfit between Rh and FCC Co is therefore +7.3%. The lattice constant of the metastable BCC phase of Co is 2.83 Å [10, 15], hence the misfit between Rh and BCC Co is −4.9%. These mismatches are rather large for pseudomorphic growth, at least by the standards of classical epitaxy theory [16], but highly strained ultrathin epitaxial films have been grown to thicknesses of the order of 10 layers in other epitaxial systems, e.g. for FCC Cu on Pd{001} [17] (misfit +7.6%) and for Fe on Rh{001} [18, 19] (misfit −6.3%).

0953-8984/93/407307+12$07.50

The Fe/Rh epitaxial system is particularly interesting because a quantitative low-energy electron-diffraction LEED analysis [18] has established that the first three layers of Fe grow pseudomorphically in the layer-by-layer mode and that the Fe film is a strained BCC phase. By contrast, a recent study of the Fe/Rh{001} system, while also reporting pseudomorphic growth (up to five layers), claims that the Fe film is a strained FCC phase (stretched 5.7% in the surface plane). We note that [18] uses the measured bulk spacing of the Fe film and the elastic constants of BCC and FCC Fe to show that the calculated strain ratio (the ratio between perpendicular bulk strain and parallel epitaxial strain) agrees with experiment only for the BCC phase. Reference [19], however, does not evaluate the bulk spacing or carry out a strain analysis to determine the equilibrium phase of the Fe film.

The case of Co on Rh{001} ought to be similar, but has not before been tested. The three questions that we address in this work are: (1) does Co grow epitaxially and pseudomorphically on Rh{001}? (2) what is the mode of growth? (3) if the answer to (1) is affirmative, what is the equilibrium (i.e. the unstrained) phase of the Co films, i.e. is it FCC or BCC?

The Rh{001} surface has been used as a substrate for epitaxial growth of a metal only in a few cases, namely: in a field-ion microscopy (FIM) study of Fe films [20]; in a study of Cu films by low-energy electron diffraction (LEED) and Auger electron spectroscopy (AES) [21]; in another study of Cu films by x-ray photoelectron spectroscopy [22]; and in LEED and AES studies of Ag films [23]. The Ag/Rh and Cu/Rh systems are typical bimetallic catalysts and are thus interesting in terms of the chemisorption of CO. The FIM study reports islands of Fe on Rh{001} after laser pulsing to 600 K, with the Fe atoms arranging themselves in a square pattern 'as expected of an epitaxial growth'. Peebles *et al* [23] found that the growth mode of Ag on Rh{001} is temperature dependent—at 300 K it is layer by layer (Frank–Van der Merwe, or FM), but at 640 K it is Stranski–Krastanov (SK). For Cu/Rh{001} pseudomorphic layer-by-layer growth is said to occur [21] up to 3 layers, although the quality of the LEED pattern above two layers is described as poor.

2. Experiments

The experiments were done in an ultrahigh-vacuum chamber capable of reaching a base pressure of 6×10^{-11} Torr and equipped with rear-view optics for the LEED studies and a double-pass cylindrical mirror analyser (CMA) for AES measurements. The Rh{001} sample was cleaned *in situ* by sputtering and annealing cycles rather than the more typical annealing in oxygen [21]. The sputtering cycles were done with 500 eV argon ions at a typical pressure of 5×10^{-5} Torr for several hours, while the subsequent annealing cycles lasted about 1 h at temperatures of approximately 600 °C. The resulting Rh{001} surface was free of any impurities to within detectable limits of our CMA, and exhibited very bright 1×1 LEED patterns up to our maximum beam energy of 512 eV.

The Co source was a 99.9965 at.% pure wire wrapped around a tungsten basket, heated resistively to typically 1300–1400 °C (as measured with an infrared pyrometer) and extensively outgassed before each deposition. Deposition rates were kept roughly constant at about 0.3 Å min^{-1} leading to pressures in the chamber of about 3×10^{-10} Torr. During deposition the Rh substrate was neither heated nor cooled—its temperature was monitored with an infrared pyrometer and was never at or above the minimum temperature measurable by this instrument (~150 °C). Previous experiments using identical sources and sample-temperature monitoring by thermocouple showed that the substrate is not significantly heated by the source during deposition.

The film thicknesses were determined from the peak-to-peak height of the Co (775 eV) and Rh (302 eV) AES signals. This standard process has been well documented before [24]. The mean free paths used in the calibration were taken from Seah and Dench [25]: 15.0 Å for the Co line and 9.4 Å for the Rh line. The thicknesses thus obtained are quoted in terms of the *layer equivalent* (LE). The conversion from ångstroms to LE was done using the relevant lattice spacings determined from the LEED intensity analyses as described below. The overall error in this thickness calibration is assumed to be ±50%, mostly derived from the choice of suitable mean free paths. Indeed, the mean free paths of Tanuma *et al* [26] are smaller than those of Seah *et al* [25] by 15% for the Co 775 eV line and 36% for the Rh 302 eV line, leading to typical errors of ±0.5 Å for a 2 Å film and ±2.5 Å for a 10 Å film.

After each deposition had been made, the film thickness was calibrated by AES and then LEED $I(V)$ curves were collected. The data-acquisition system consists of a TV camera linked via a digitizer card to a microcomputer [27]. The software typically allows for the collection of all degenerate 10, 11, 20, 21, and 22 beams within about 1 h for very good statistics. The LEED patterns and the associated $I(V)$ spectra were all totally reproducible for similar film thicknesses on different occasions and for different deposition rates.

3. Observations

The changes in the LEED patterns with increasing deposition of Co on the Rh{001} surface were very similar to those observed in the study of Fe on Rh{001} as reported elsewhere [18]. A very good 1 × 1 pattern from the clean substrate gradually became slightly more diffuse with increasing coverage as the background increased. The pattern remained 1 × 1 throughout. The signal-to-background ratio worsened with coverage to such an extent that the thickest film for which $I(V)$ data could be taken was about 8–10 LE. The corresponding beams were quite broad and diffuse, albeit still bright, on a fairly high background. No change in the angular positions of the LEED 1 × 1 pattern at a given energy was observed with increasing film thickness within the angular resolution of the observations of about 1%.

The evolution of the 10 and 11 spectra with increasing surface coverage can be seen in figure 1 parts (*a*) and (*b*), respectively. The curves from the clean Rh{001} substrate (labelled 0 LE) compare perfectly with those taken in previous experiments [18] and with curves taken from very thick unstrained Rh on Au{001} [28], as well as with curves measured on clean Rh{001} by Oed *et al* [29]. Figure 1 shows that the curves monitored around the monolayer level are distinctly different from those from the clean substrate, indicating ordered growth. With increasing surface coverage gradual changes occur until stabilization is reached with the thickest films grown, i.e. above about 6 LE. This observation, together with the persisting 1 × 1 geometry of the LEED pattern, suggests pseudomorphism up to the thickest films studied. Whether the growth mode is layer by layer remains to be proven.

4. LEED intensity analyses

In view of the good quality of the 1 × 1 LEED patterns and of the gradual changes in the $I(V)$ spectra with coverage in the early stages of growth, it is appropriate to test whether some of the curves can be fitted by intensity calculations of models involving complete pseudomorphic layers. The intensity calculations were performed with Jepsen's

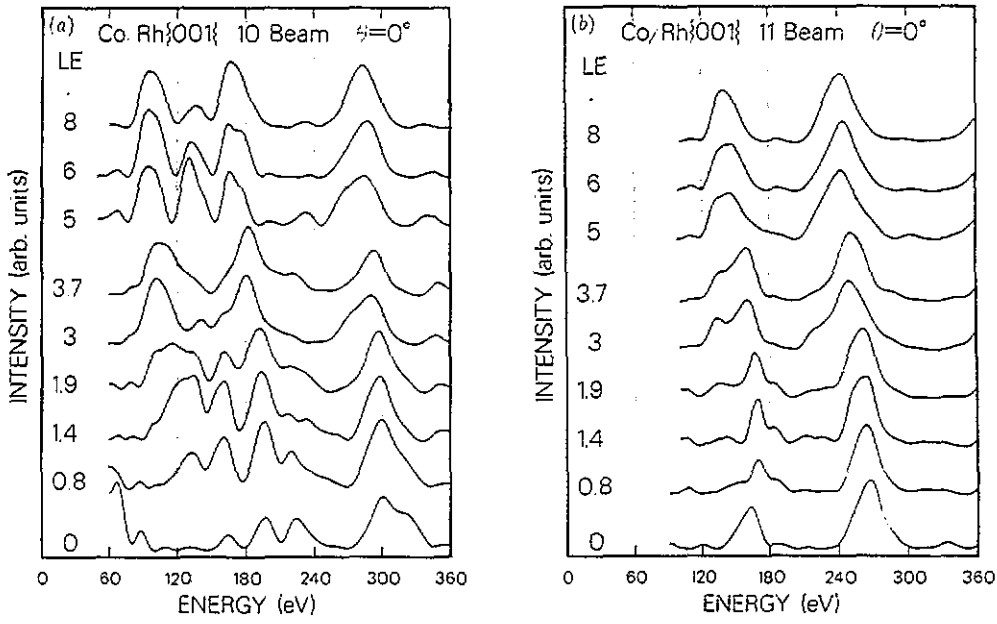

Figure 1. Evolution of the (*a*) 10 and (*b*) 11 spectra for Co on Rh{001} with increasing film thickness given in LE.

full-dynamical CHANGE program [30] and the following non-structural parameters: Rh and Co potentials taken from the collection of Moruzzi *et al* [31]; eight phase shifts and 69 beams up to 500 eV; inner potential $V_0 = -(10 + 4i)$ eV, with the real part adjustable in the fitting process; and an isotropic root-mean-square amplitude of thermal vibrations of 0.15 Å. Evaluation of the agreement between theoretical and experimental curves was done both visually and by *R*-factor analysis. Three *R* factors were used, namely, the Van Hove–Tong R_{VHT} [32], the Zanazzi–Jona r_{ZJ} [33] and the Pendry R_P [34] factors.

4.1. The first layer

It is noticeable in figure 1 that the 10 and the 11 spectra for 0.8 LE and 1.4 LE films are quite similar to each other, but both are distinctly different from the clean Rh{001} curves. Since the errors in the thickness calibration are estimated to be at least ±50%, we have compared the curves calculated for a Co monolayer at various distances from the Rh surface with both sets of experimental data. The Co–Rh interlayer spacing was varied in the initial stages between 1.40 and 1.80 Å in steps of 0.05 Å, and in the refinement stage between 1.70 and 1.86 Å in steps of 0.02 Å. Best agreement (both by visual evaluation and by all three *R* factors) was found between the experimental data from the 1.4 LE film and a pseudomorphic Co monolayer at a distance of 1.77±0.03 Å from the Rh{001} surface. The corresponding *R* factors are $R_{VHT} = 0.27$, $r_{ZJ} = 0.12$ and $R_P = 0.35$. The quality of the fit can be judged from figure 2.

4.2. The second layer

From inspection of the $I(V)$ spectra of the 1–4 LE films of Co (nominal thicknesses determined by AES) in figure 1 it is evident that the curves for the 3.0 LE film show larger

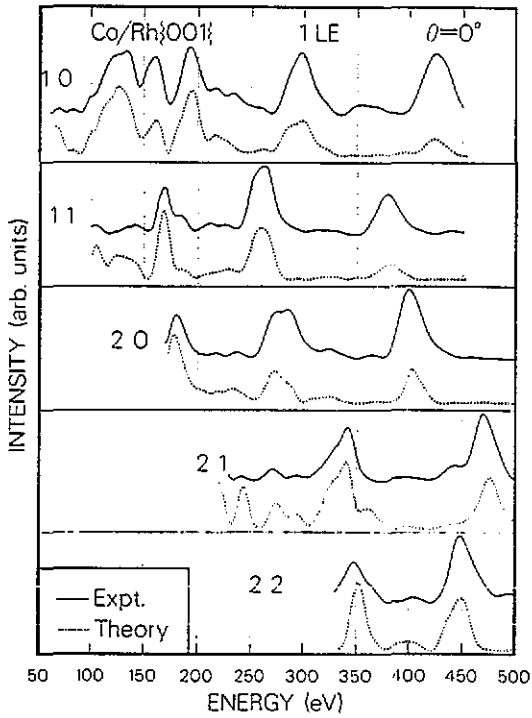

Figure 2. Normal-incidence experimental (full curves) and theoretical (broken curves) $I(V)$ spectra for a pseudomorphic monolayer of Co on Rh{001}.

changes when compared to the monolayer model than those from the 1.9 LE film. The 3.0 LE film is thus more likely to fit a two-layer model than the 1.9 LE film, but both sets of experimental data were tested. In the process of developing a two-layer model to fit the experiment the problem is to identify both the first and the second interlayer spacings, i.e. d_{Co-Co} and d_{Co-Rh}, respectively. We varied d_{Co-Co} from 1.40 to 1.80 Å in steps of 0.05 Å and for each value of d_{Co-Co} we varied d_{Co-Rh} from 1.6 to 2.0 Å in steps of 0.05 Å.

In trying to fit the experimental data we found that the $I(V)$ spectra from the nominal 1.9 LE film could not possibly match the curves calculated for a two-layer film, whereas the curves from the nominal 3 LE film were in good visual agreement with the calculated spectra. However, the R-factor analysis of the 3 LE film produced contradictory results: each of the three R factors used was minimized with different sets of structural parameters—ranging from 1.61 to 1.68 Å for d_{Co-Co} and from 1.77 to 1.80 Å for d_{Co-Rh}, as shown by the contour plots in figure 3. The $I(V)$ spectra calculated for each of the three sets of parameters were in fact visibly different from one another and only in fair agreement with experiment. Figure 4 shows the curves calculated for a set of parameters ($d_{Co-Co} = 1.65$ Å, $d_{Co-Rh} = 1.80$ Å—broken curves labelled 'theory 1' in the figure) that corresponds to the average of the values that minimize the three R factors. By contrast, we also show in figure 4 the $I(V)$ curves ed as best fitting by visual evaluation (dotted curves labelled 'theory 2'): these curves were calculated with the values $d_{Co-Co} = 1.60$ Å and for $d_{Co-Rh} = 1.75$ Å. The agreement is visually good, certainly better than that of 'theory 1'. We therefore conclude that the structural parameters of the two-layer Co film are, with somewhat larger error bars, $d_{Co-Co} = 1.60 \pm 0.04$ Å and $d_{Co-Rh} = 1.75 \pm 0.04$ Å. The corresponding R-factor values are $R_{VHT} = 0.43$, $r_{ZJ} = 0.18$ and $R_P = 0.43$.

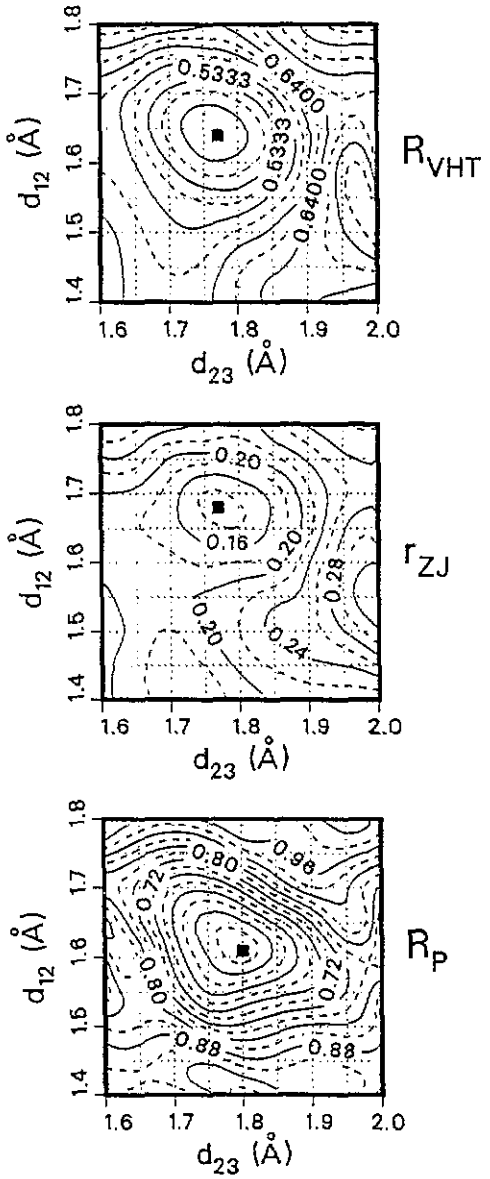

Figure 3. *R*-factor contour plots in the plane of interlayer spacings $d_{12} = d_{Co-Co}$ versus $d_{23} = d_{Co-Rh}$ for a two-layer film of Co on Rh{001}. See the text for the best-fit parameter values.

4.3. The thick film

Although the thickest Co film for which LEED intensity data were collected in this work was about 10 LE thick, the corresponding LEED pattern (as well as that of 8 LE films) exhibited high background and broad spots, and the $I(V)$ spectra were very noisy. We decided therefore, in order to study the crystallographic properties of 'thick' films, to try and fit the intensity data collected from a 6 LE film, which produced a brighter and sharper LEED pattern. The differences between the $I(V)$ spectra from films thicker than 6 LE are small

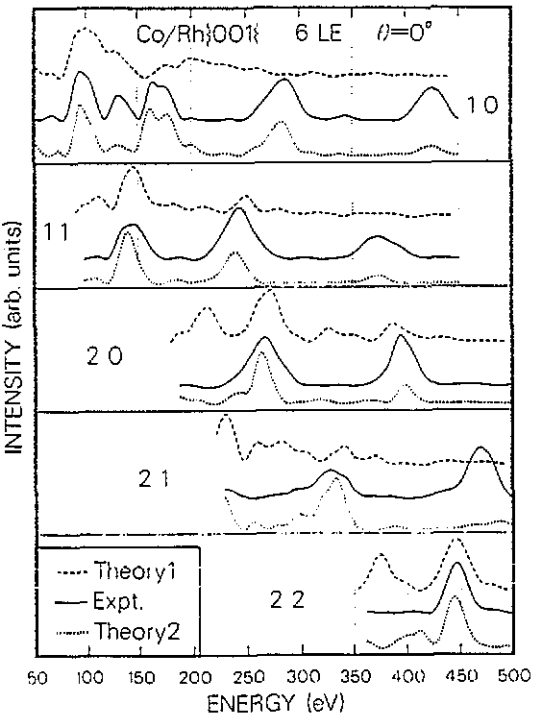

Figure 4. Experimental (full curves) and theoretical $I(V)$ spectra for a pseudomorphic bilayer of Co on Rh{001}. Theory 1 used average values of the parameters that minimize the R-factors (broken curves). Theory 2 used parameters that produced $I(V)$ curves (dotted) with the best visual fit to experiment.

in any case, as can be seen for the 10 and the 11 curves from 6 and 8 LE films in figure 1.

Since a 6- or 8-layer film is practically semi-infinite for electrons with energies smaller than 500 eV, the calculations were done for a semi-infinite Co{001} crystal with the in-plane mesh constant of Rh{001}, i.e. $a = 2.69$ Å. The variables in these calculations were the bulk interlayer spacing d_{bulk}, the first interlayer spacing d_{12} and, if needed, the second interlayer spacing d_{23}. In the first stage d_{bulk} was varied between 1.45 and 1.75 Å in steps of 0.05 Å, and in the refinement stage it was varied between 1.51 and 1.63 Å in steps of 0.02 Å. For each value of d_{bulk}, the *change* Δd_{12} in the first interlayer spacing d_{12} was varied from a contraction of 0.2 Å to an expansion of 0.2 Å in steps of 0.05 Å. The contour plots of the three R-factors used are depicted in figure 5, and show that while all three R-factors are minimized for $d_{\text{bulk}} = 1.60$ Å, discrepancies occur concerning the value of Δd_{12}, for which R_{VHT} and r_{ZJ} select -0.15 Å and R_{P} selects 0.02 Å. The visual evaluation finds the best fit with the curves calculated for $d_{\text{bulk}} = 1.60$ and $\Delta d_{12} = 0.05$ Å. These curves are drawn dotted and labelled 'theory 2' in figure 6, where they are compared to the experimental intensities (full curves). For comparison, we also show in figure 6 the curves calculated for $d_{\text{bulk}} = 1.60$ and $\Delta d_{12} = -0.15$ Å (broken curves labelled 'theory 1'). The fit achieved with 'theory 2' is good, and we quote the final results as $d_{\text{bulk}} = 1.60 \pm 0.03$ Å and $\Delta d_{12} = 0.05 \pm 0.03$ Å.

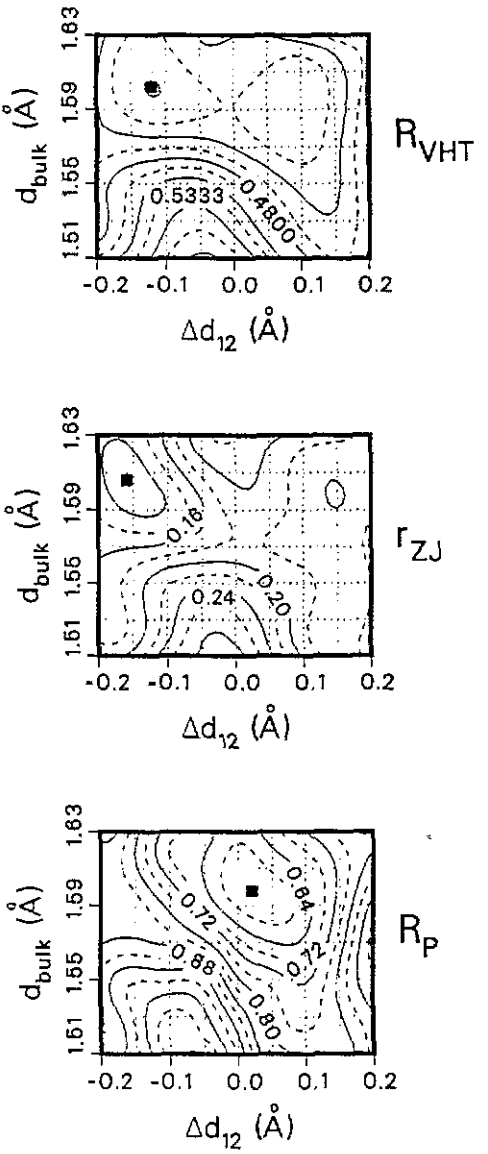

Figure 5. *R*-factor contour plots in the plane of interlayer spacings d_{bulk} versus d_{12} for an eight-layer film of Co on Rh{001}. See the text for the best-fit parameter values.

5. Strain analysis

The results of the LEED experiment and of the LEED intensity analyses can be used to determine the equilibrium (i.e. the unstrained) phase of, and hence the strains in, the Co films grown. The structure of these films, as determined above, is body-centred tetragonal with lattice parameters $a = 2.69$ Å and $c = 2d_{bulk} = 3.20$ Å.

We are interested in the ratio between the strain ϵ_3 in the direction perpendicular to the film and the linear strain ϵ_1 in the plane of the film—the so-called strain ratio. We write

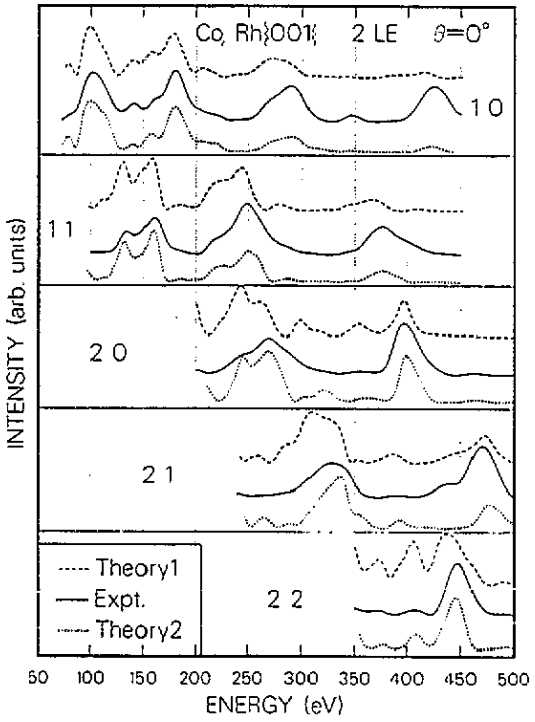

Figure 6. Experimental (full curves) and theoretical $I(V)$ spectra for a 6 LE film of Co on Rh{001}. Theory 1 used average values of the parameters that minimize the R-factors (broken curves). Theory 2 used parameters that produced $I(V)$ curves (dotted) with the best visual fit to experiment.

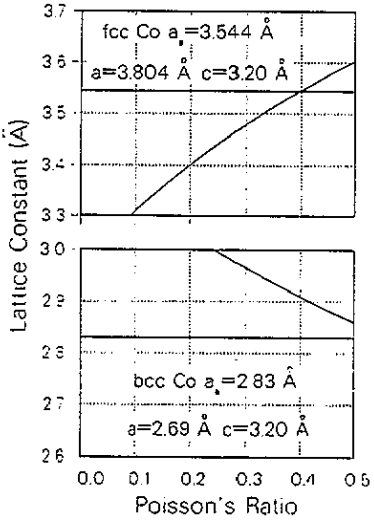

Figure 7. Plot of a_{eq} versus Poisson's ratio ν (see (2) in the text) for the assumptions that the equilibrium phase is FCC Co (top curve) or BCC Co (bottom curve).

this strain ratio as

$$\epsilon_3/\epsilon_1 = r_s = \left[(c - c_{eq})/c_{eq}\right] / \left[(a - a_{eq})/a_{eq}\right] \tag{1}$$

where c_{eq} and a_{eq} are the lattice parameters of the equilibrium phase; the denominator is the misfit between the substrate and the equilibrium phase. The LEED results (the a and c values) allow us to calculate r_s if the equlibrium phase is known. In the present case we have two choices for the equilibrium phase, both metastable: either FCC Co or BCC Co.

If the equilibrium phase is FCC Co ($a_0 = 3.544$ Å [14]) then $a_{eq} = a_0/\sqrt{2} = 2.506$ Å and $c_{eq} = 3.544$ Å, and therefore $r_s = -1.32$. If the equilibrium phase is BCC Co ($a_0 = 2.83$ Å [15]) then $a_{eq} = c_{eq} = 2.83$ Å, and therefore $r_s = -2.64$. If we knew the elastic constants of both phases we could identify the equilibrium phase, since the value of the strain ratio on cubic {001} can be shown by linear elasticity theory [35] to be $r_s = -2c_{12}/c_{11}$, with c_{12} and c_{11} being the elastic constants. However, we do not know the elastic constants of FCC and BCC Co.

Fortunately, there is another approach. The strain ratio can be related directly to Poisson's ratio ν, as $r_s = -2\nu/(1-\nu)$, so that we can rewrite (1) in the form [35]:

$$a_{eq} = [2\nu/(1+\nu)]\,a + [(1-\nu)/(1+\nu)]\,c. \tag{2}$$

With known a and c we can calculate the expression on the right-hand side for several values of ν and plot it on a graph of a_{eq} versus ν, as in figure 7. Thus we obtain an FCC-Co curve by using $a = 3.804$ Å and $c = 3.20$ Å, and a BCC-Co curve by using $a = 2.83$ Å and $c = 3.20$ Å. The plot shows that there are no physically acceptable values of the Poisson ratio that would satify (2) with $a_{eq} = 2.83$ Å, i.e. that the BCC line does not intersect the horizontal line at 2.83 within the range of acceptable ν values. The FCC line, however, does cross the horizontal line drawn at the value 3.544 of the lattice constant of FCC Co in the acceptable range, the intersection being at $\nu = 0.4$. This value of Poisson's ratio is larger than that found in the literature (0.32 for HCP Co [36]). It could be that Poisson's ratio for FCC Co is indeed 0.4, or that the limits of linear elasticity theory are exceeded, but in any case it seems established that the equilibrium phase of the films grown in these experiments was not BCC Co, but rather FCC Co.

The strains in the films are therefore known: in the plane of the films there is a 7.3% expansion due to the misfit between the lattice constants of the Rh substrate (3.804 Å) and FCC Co (3.544 Å), while in the perpendicular direction there is a 9.7% contraction caused by the in-plane epitaxial strain. These strains are very large by metallurgical standards.

6. Discussion and conclusion

The present work has shown the following.

(1) Ultrathin epitaxial Co films grow pseudomorphically on Rh{001}, i.e. the films assume the same interatomic spacing in the plane of the films as the substrate.

(2) Co wets the surface of the substrate. This result is not too surprising in view of the relative magnitudes of the surface free energies of substrate and film (2.828 J m^{-2} for Rh and 2.709 J m^{-2} for Co [37]). As a consequence, the Co films grow in the layer-by-layer mode for at least the first two layers, as proven directly by LEED structure analysis. The monolayer is 1.77 ± 0.03 Å distant from the Rh{001} surface. This interlayer spacing does not change much for the bilayer (1.75 ± 0.04 Å), but the interlayer spacing between the two Co layers is 1.60 ± 0.04 Å.

(3) The atomic structure of the Co films is a strained modification of the (high-temperature) FCC phase of Co. Thick films have the following crystallographic parameters: the in-plane lattice constant is 2.69 Å (forced by the Rh{001} substrate), the bulk interlayer spacing is 1.60 ± 0.03 Å and the first interlayer spacing is 1.65 ± 0.04 Å. The strains in the films are very large: +7.3% in the plane and −9.7% in the perpendicular direction. It may be noted that the FCC phase is favoured over the metastable BCC phase of Co despite the fact that for the latter the misfit is (at −4.9%) smaller, albeit compressive, than that of FCC Co. Note that Co, in contrast to the case for Fe, chooses the FCC phase rather than the BCC phase on Rh{001}, even though the mismatch of BCC Co (−4.9%) is less than that of BCC Fe (−6.3%). However, BCC Co is much less stable than FCC Co, in contrast to Fe, and requires a much closer lattice match to stabilize. Films thicker than about 10 layers exhibit less and less long-range order, undoubtedly caused by increasing numbers of misfit dislocations.

(4) The volume per atom is 11.128 $Å^3$ in the equilibrium phase (FCC Co) and 11.576 $Å^3$ in the bulk of the Co films—an increase of 3.9%. We can therefore speculate that the films would exhibit an enhanced magnetic moment with respect to the unstrained phase. The 3% expansion of the first spacing over the bulk spacing of the Co film indicates a larger magnetic moment on the Co first layer, hence larger atomic size of the first-layer atoms, as one would expect from the decreased coordination. The situation for Fe films is similar.

A final comment of interest to LEED crystallographers concerns the differences between the structural parameters that minimize different R-factors. We have noted repeatedly before [38–40] that different R-factors can sometimes lead to different structures (different in the sense that the corresponding 'best-fit' parameters are outside the error bounds), and that some of these structures may not be quite acceptable to a visual evaluation of the fit. We believe that the best protections against these pitfalls are to use more than one R-factor in the search for the 'best' fit to experiment and to keep visual inspection as a necessary component of LEED intensity analysis.

Acknowledgments

This work was sponsored in part by the National Science Foundation with Grant DMR8921123 and by the Department of Energy with Grant DE- FG0286-ER45239.

References

[1] Lin C J, Gorman G L, Lee C H, Farrow R F C, Marinero E E, Do H V, Notarys H and Chien C J 1991 *J. Magn. Magn. Mater.***93** 194
[2] den Broeder F J A, Kuiper D, Donkersloot H C and Hoving W 1989 *Appl. Phys.* A **49** 507
[3] Engel B N, England C D, Van Leeuwen R A, Wiedmann M H and Falco C M 1991 *Phys. Rev. Lett.* **67** 1910
[4] Pescia D, Zampieri G, Stampanoni M, Bona G L, Willis R F and Meier F 1987 *Phys. Rev. Lett.* **58** 933
[5] Lee C H, He H, Lamelas F, Vavra W, Uher C and Clarke R 1989 *Phys. Rev. Lett.* **62** 653; 1990 *Phys. Rev.* B **42** 1066
[6] de Miguel J J, Cebollada A, Gallego J M, Miranda R, Schneider C M, Schuster P and Kirschner J 1991 *J. Magn. Magn. Mater.* **93** 1
[7] Clarke A, Jennings G, Willis R F, Rous P J and Pendry J B 1987 *Surf. Sci.* **187** 327
[8] Li H and Tonner B P 1990 *Surf. Sci.* **237** 141
[9] Chambers S A, Anderson S B, Chen H-W and Weaver J H 1987 *Phys. Rev.* B **35** 2592
[10] Prinz G A 1985 *Phys. Rev. Lett.* **54** 1051
Krebs J J 1989 *Appl. Phys.* A **49** 513
[11] Idzerda Y U, Elam W T, Jonker B T and Prinz G A 1989 *Phys. Rev.* B **62** 2480
[12] Li H and Tonner B P 1989 *Phys. Rev.* B **40** 10241
[13] Scheurer F, Carrière B, Deville J P and Beaurepaire E 1991 *Surf. Sci. Lett.* **245** L175
[14] Pearson W B 1967 *A Handbook of Lattice Spacings and Structures of Metals and Alloys* vol 2 (New York: Pergamon)
[15] Marcus P M and Moruzzi V L 1985 *Solid State Commun.* **55** 971
[16] Jesser W A and van der Merwe J H 1989 *Dislocations in Solids* ed F R N Nabarro (Amsterdam: Elsevier) ch 41
[17] Li H, Wu S C, Tian D, Quinn J, Li Y S, Jona F and Marcus P M 1989 *Phys. Rev.* B **40** 5841
[18] Begley A M, Kim S K, Jona F and Marcus P M 1993 *Phys. Rev.* B **48** 1786
[19] Egawa C, Tezuka Y, Oki S and Murata Y 1993 *Surf. Sci.* **283** 338
[20] Gao Q J and Tsong T T 1987 *Surf. Sci.* **191** L787
[21] Jiang X and Goodman D W 1991 *Surf. Sci.* **255** 1
[22] Rodriguez J A, Campbell R A and Goodman D W 1991 *J. Phys. Chem.* **95** 2477
[23] Peebles H C, Beck D D, White J M and Campbell C T 1985 *Surf. Sci.* **150** 120
[24] See, for example, Quinn J, Li Y S, Li H, Tian D, Jona F and Marcus P M 1991 *Phys. Rev.* B **43** 3959
[25] Seah M P and Dench W A 1986 *Surf. Interface Anal.* **1** 2
Seah M P 1986 *Surf. Interface Anal.* **9** 85
[26] Tanuma S, Powell C J and Penn D R 1998 *Surf. Interface Anal.* **11** 577; 1990 *J. Vac. Sci. Technol.* A **8** 2213
[27] Jona F, Strozier J A Jr and Marcus P M 1985 *The Structure of Surfaces* ed M A Van Hove and S Y Tong (Berlin: Springer) p 92
[28] Li H, Wu S C, Tian D, Li Y S, Quinn J and Jona F 1991 *Phys. Rev.* B **44** 1438

[29] Oed W, Dötsch B, Hammer L, Heinz K and Molar K 1988 *Surf. Sci.* **207** 55
[30] Jepsen D W 1980 *Phys. Rev.* B **22** 5701; 1980 *Phys. Rev.* B **22** 814
[31] Moruzzi V L, Janak J F and Williams A R 1978 *Calculated Electronic Properties of Metals* (New York: Pergamon)
[32] Van Hove M A, Tong S Y and Elconin M H 1977 *Surf. Sci.* **64** 85
[33] Zanazzi E and Jona F 1977 *Surf. Sci.* **62** 61
[34] Pendry J B 1980 *J. Phys. C: Solid State Phys.* **13** 937
[35] Jona F and Marcus P M 1991 *Surface Physics and Related Topics* ed Fu-Jia Yang, Guang-Jiong Ni, Xun Wang, Kai-Ming Zhang and Dong Lu (Singapore: World Scientific) p 213
[36] *Smithells Metals Reference Book* 6th edn, ed Eric A Brandes (London: Butterworths) pp 15-2
[37] Mezey L Z and Giber J 1982 *Jpn. J. Appl. Phys.* **21** 1569
[38] Li Y S, Quinn J, Li H, Tian D, Jona F and Marcus P M 1991 *Phys. Rev.* B **44** 8261
[39] Begley A M, Kim S K, Quinn J, Jona F, Over H and Marcus P M 1993 *Phys. Rev.* B **48** 1779
[40] Jona F 1987 *Surf. Sci.* **192** 398, 414